



*Search for deviations*  
**within the EFT framework**  
**at ATLAS and CMS**

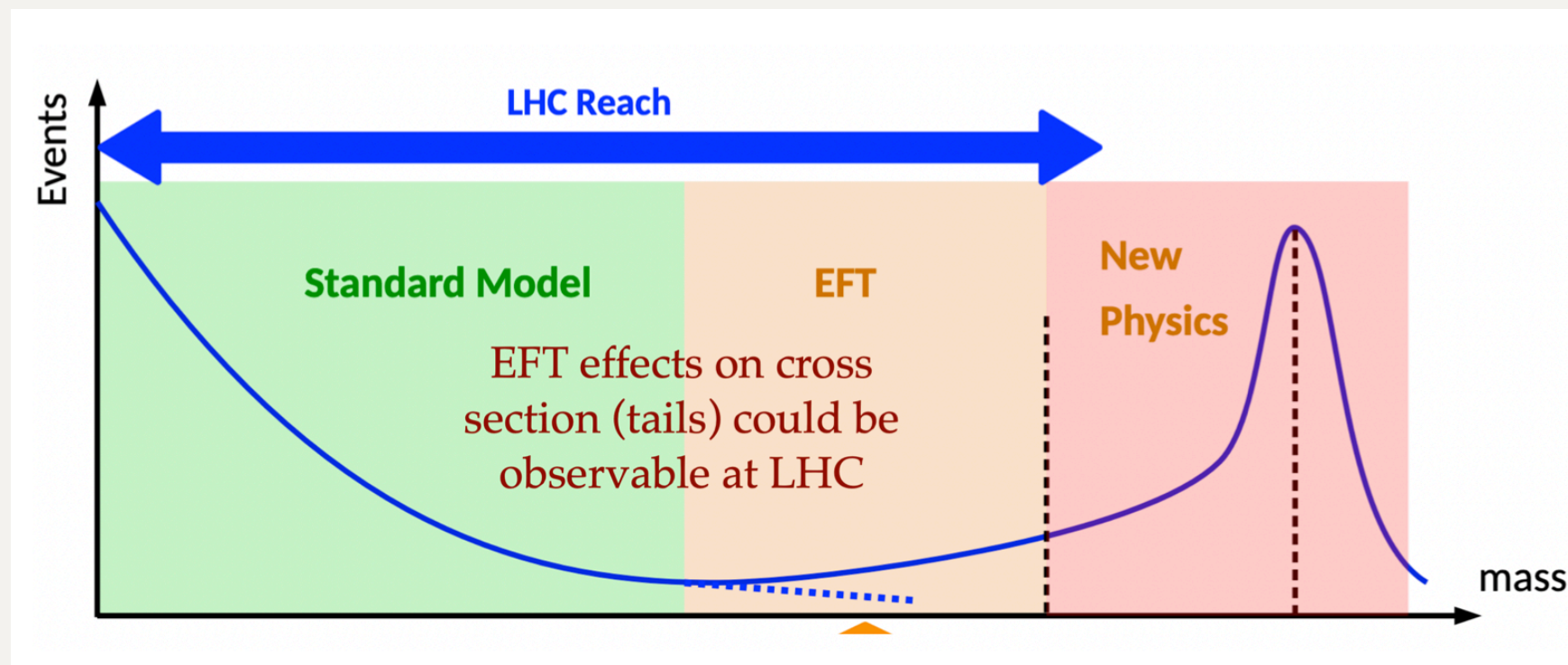
**Tina Ojeda**

on behalf of the ATLAS & CMS collaborations

60th Rencontres de Moriond on  
Electroweak Interactions & Unified Theories  
March 19, 2026

# Introduction

- Searches for phenomena beyond the SM important part of physics programme at the LHC
  - Direct searches, e.g. “bump hunt”
  - Indirect searches → look for deviations from SM in various measurements
- No new particle discovered (yet)
  - New heavy particles beyond reach of LHC could distort lower-energy physics
  - Potential effect of new heavy particles parametrised within EFT framework
    - Fairly model independent



# (SM)EFT

- Extends SM Lagrangian by introducing terms of higher dimension

Wilson coefficient  $c_i$

$$\mathcal{L}_{\text{SMEFT}} = \mathcal{L}_{\text{SM}} + \sum_i \frac{c_i^{(5)}}{\Lambda} Q_i^{(5)} + \sum_i \frac{c_i^{(6)}}{\Lambda^2} Q_i^{(6)} + \sum_i \frac{c_i^{(7)}}{\Lambda^3} Q_i^{(7)} + \sum_i \frac{c_i^{(8)}}{\Lambda^4} Q_i^{(8)} + \dots$$

Scale of “new physics”  $\Lambda$ , usually set to 1 TeV

- Terms of  $d = 5, 7$  violate lepton/baryon number conservation
  - Not usually considered
- **Leading order contributions from  $d = 6$** 
  - Incomplete description of  $d = 8$

# (SM)EFT

- Have terms that are linear/quadratic in new operators

$$|\mathcal{M}_{\text{SMEFT}}|^2 = |\mathcal{M}_{\text{SM}}|^2 + 2 \sum_i \frac{c_i}{\Lambda^2} \text{Re}(\mathcal{M}_{\text{SM}}^* \mathcal{O}_i) + \sum_{i,j} \frac{c_i c_j}{\Lambda^4} (\mathcal{O}_i^* \mathcal{O}_j)$$

$$\sigma_{\text{SMEFT}} = \sigma_{\text{SM}} + \sigma_{\text{int}} + \sigma_{\text{BSM}}$$

- **Linear**  $\rightarrow$  SM/BSM interference  $\mathcal{O}(\Lambda^{-2})$
- **Quadratic**  $\rightarrow$  pure BSM effects  $\mathcal{O}(\Lambda^{-4})$ , including cross-terms
  - Same order as linear terms for  $d = 8$

Goal: use LHC data to place constraints on various Wilson coefficients

- Design analyses to be sensitive to some (set of)  $c_i$
- Re-interpret measurements to place constraints on  $c_i$  (usually cross-sections)

# Measurements

## Electroweak

  $Z\gamma$  [arXiv:2512.08582]

 VBF +  $2j$  [arXiv:2510.00118]

 VBS +  $VVV$  [CERN-EP-2026-076] **NEW**

  $WW$  photon-fusion production [arXiv:2601.21574]

  $\gamma + 2j$  [arXiv:2512.00502]

  $W\gamma$  [CERN-EP-2026-078] **NEW**

  $VVV$  [CMS-PAS-SMP-24-017] (in backup)

+  Global EFT fit  
[arXiv:2504.02958]

## Higgs

  $H \rightarrow WW^*$  [arXiv:2504.07686]

  $H \rightarrow WW^*$  [arXiv:2509.07958]

  $H, HH$  combinations [arXiv:602.18611,  
arXiv:2510.07527] ( $HH$  in backup)

  $HH \rightarrow b\bar{b}\gamma\gamma$  [ATL-PHYS-PUB-2025-034] (in backup)

  $t\bar{t}HH$  [arXiv:2603.13113] \* **NEW**

## Top

 Differential t-channel single top [arXiv:2601.04938, arXiv:2510.23372]

  $t\bar{t}$  rapidity + charge asymmetry [ATL-PHYS-PUB-2025-037]

  $t\bar{t}Wj_{EW}$  [arXiv:2509.19038]

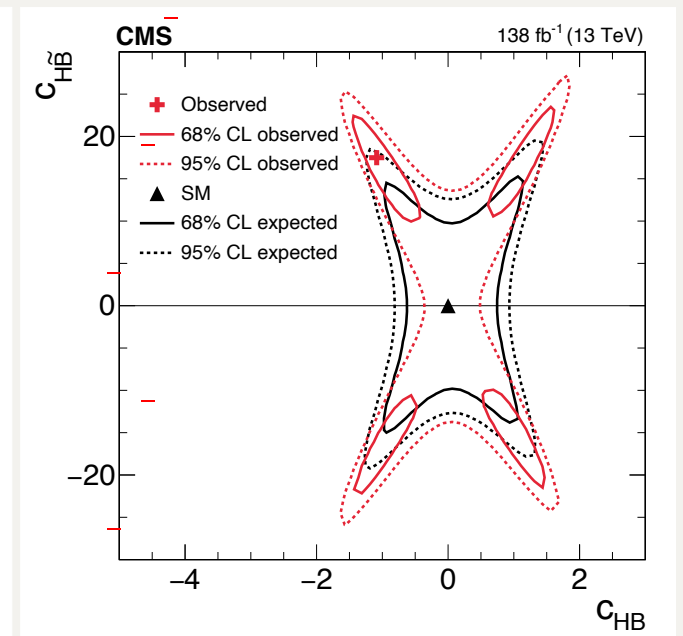
  $t\bar{t}Z + VZ$  [arXiv:2507.17498] \*

  $ttt, t\bar{t}\bar{t}$  [CMS-PAS-TOP-24-008] \*

 CP violation in  $t\bar{t}Z, tZq$  [arXiv:2505.21206] \*

# Higgs sector: $HVV$

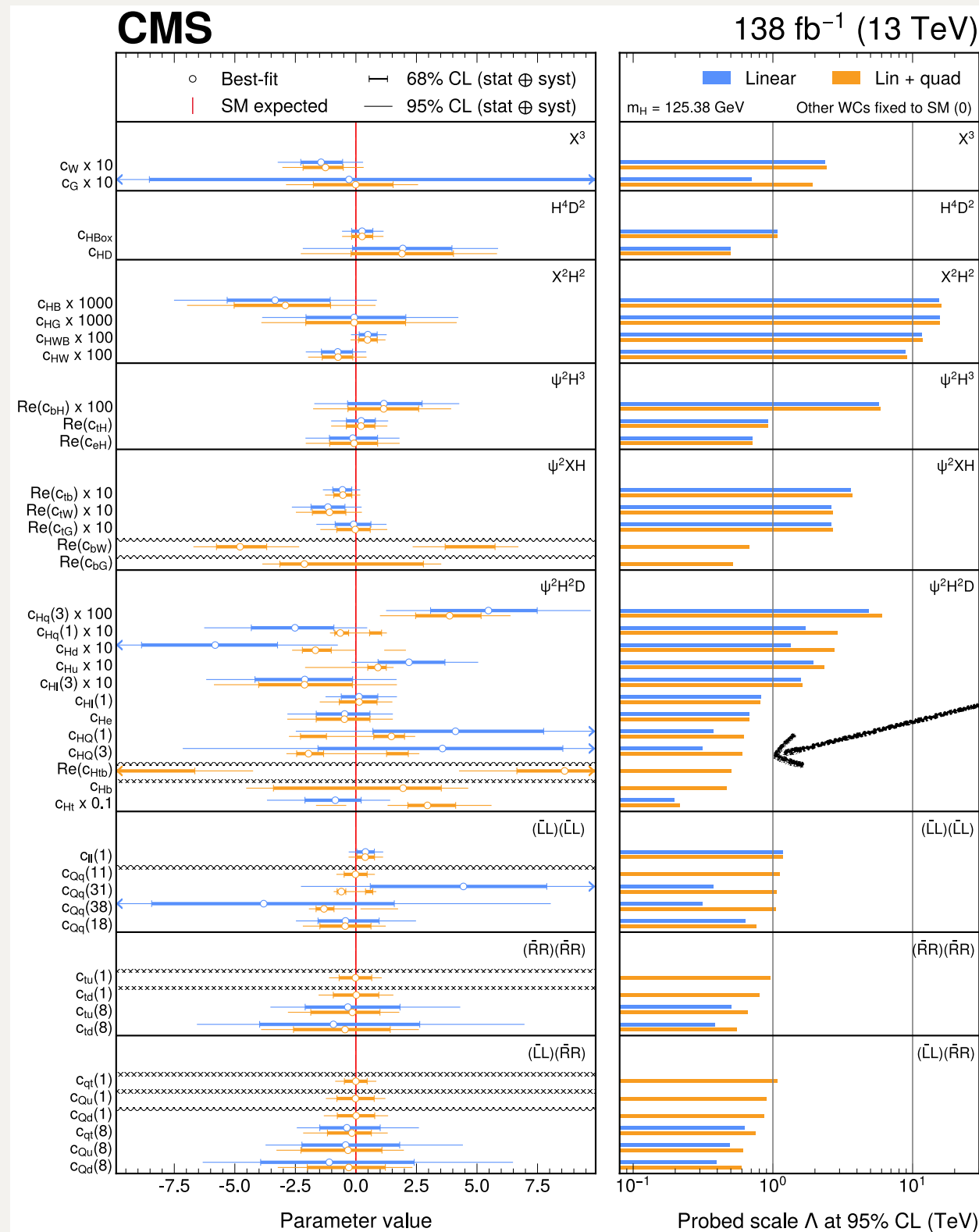
- $HVV$  interaction ( $ggH$ ,  $VBFH$  production and  $H \rightarrow WW^*$  decay)
  - CP-odd + CP-even  $\rightarrow$  different effects on distributions e.g.  $\Delta\phi_{jj}$
  - Dominated by  $d = 6$  terms
- CMS: ADNN to reduce model dependence
  - Goals: s/b + similar output for varied samples (e.g.  $c \neq 0$ )
    - Residual model dependence: acceptance effects
  - **All results consistent with SM**
  - Slight excess ( $\sim 2\sigma$  local, 14 operators) for  $c_{HB}, c_{H\tilde{B}}$
- ATLAS: STXS measurements as input
  - No 2D  $c_{HB}, c_{H\tilde{B}}$ , but no excess in standalone  $c_{HB}$ 
    - **All results compatible with SM**



# Higgs sector: combinations

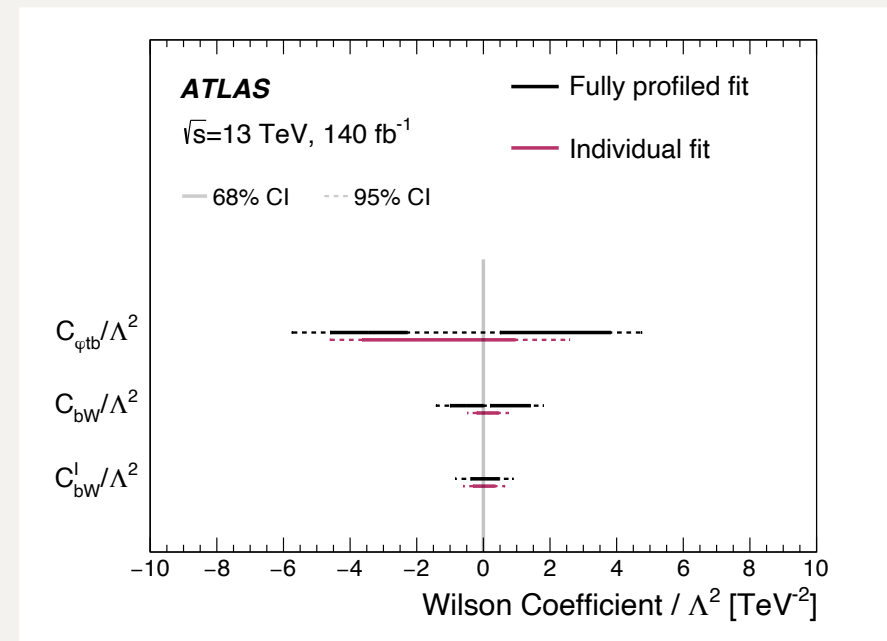
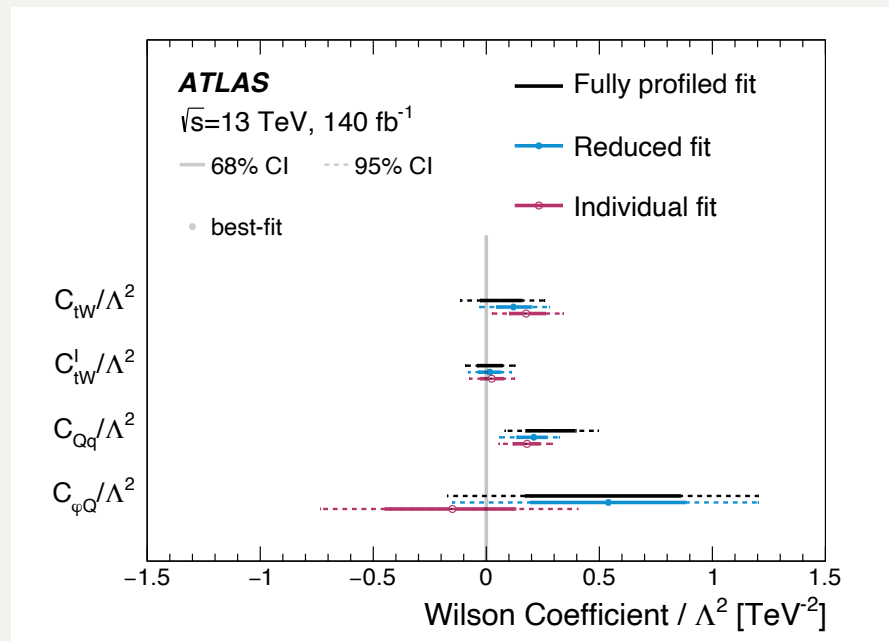
- EFT interpretations in  $H$  STXS stage 1.2 combination
  - topU3l to impose flavour symmetry + only CP-conserving operators
  - Sensitivity to 43 (out of 129) remaining operators  $\rightarrow$  similar number for ATLAS (46)  
[arXiv:2402.05742]
- Efficiency for STXS bins  $\sim$  flat wrt EFT operators
  - Not true for 4-body decays ( $H \rightarrow ZZ^* \rightarrow 4\ell, H \rightarrow WW^* \rightarrow \ell\nu\ell\nu$ )
    - Lack of fiducial phase space restriction on final-state particles in STXS
  - Re-weighting of partial decay widths implemented
- Tightest constraints on  $c_{HG}$  and  $c_{HB}$  from  $ggH$  and  $H \rightarrow \gamma\gamma$  respectively (around 15 TeV)
- **All results agree with SM** ( $p_{SM} = 0.11$ )
- $HH$  EFT interpretations with focus on  $c_{tthh'}$ , see backup

# Higgs sector: combinations

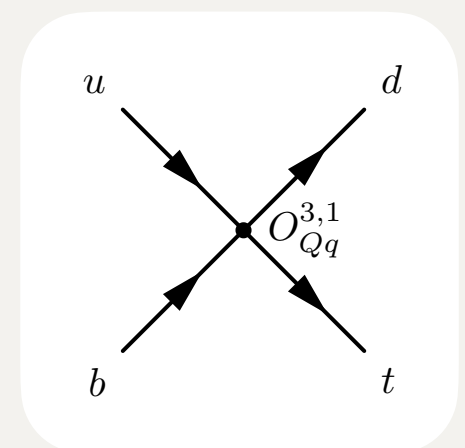


# Top sector: single top

- Decay: study of 4 angles that define  $t \rightarrow Wb$  decay
  - $\theta_W, \phi_W$  in  $t$  rest frame;  $\theta_\ell, \phi_\ell$  in  $W$  rest frame
  - Total systematic uncertainty dominant**



- Production :  $p_T(t, \bar{t})$  unfolded distributions
  - $c_{Qq}^{3,1} \neq 0 \rightarrow$  harder spectrum
  - 95%CL:  $-0.12 \text{ TeV}^{-2} < c_{Qq}^{3,1}/\Lambda^2 < 0.12 \text{ TeV}^{-2}$** 
    - No deviation in previous measurement [\[arXiv:2403.02126\]](https://arxiv.org/abs/2403.02126):  
 $-0.87 < c_{Qq}^{3,1}/\Lambda^2 < 1.42$



# Top sector: $t\bar{t}$

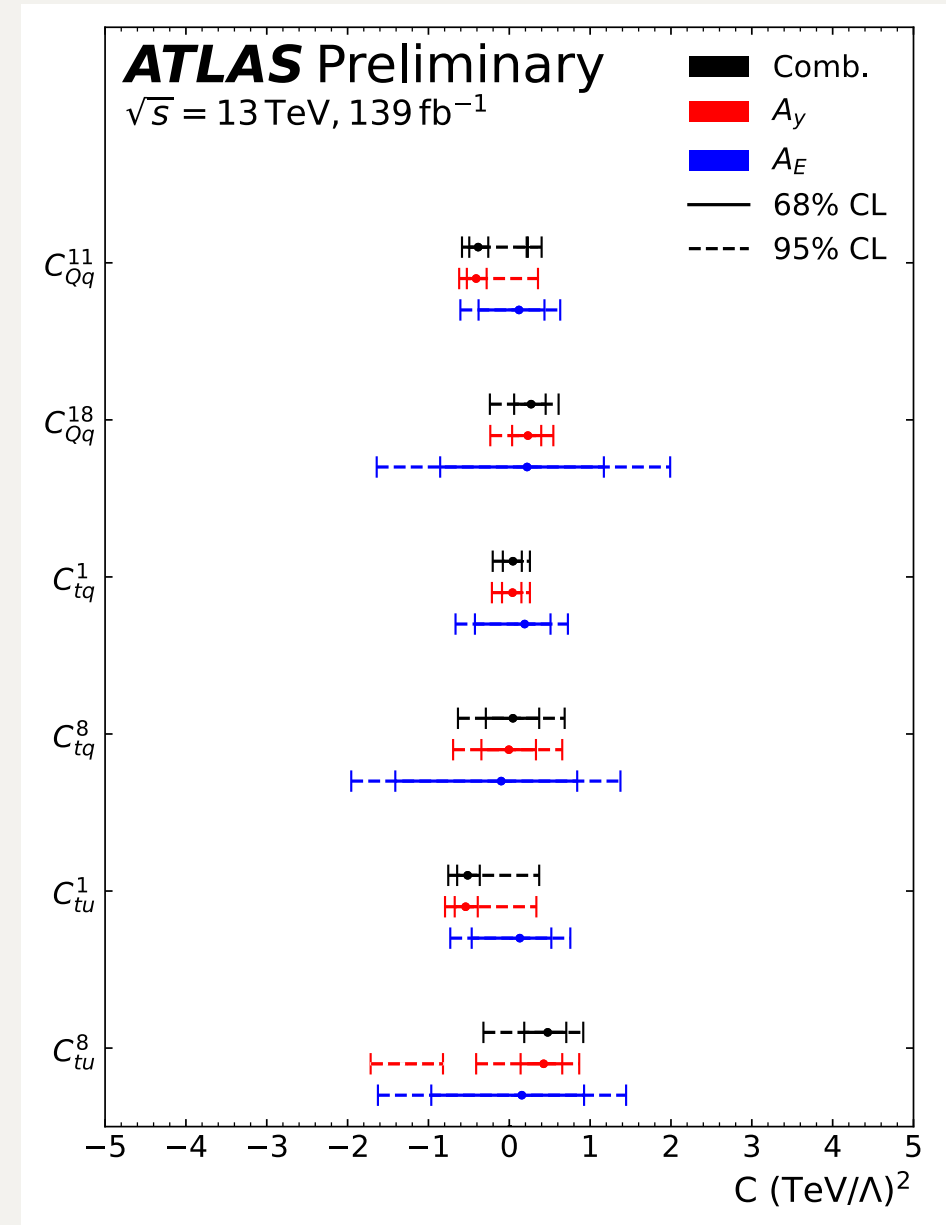
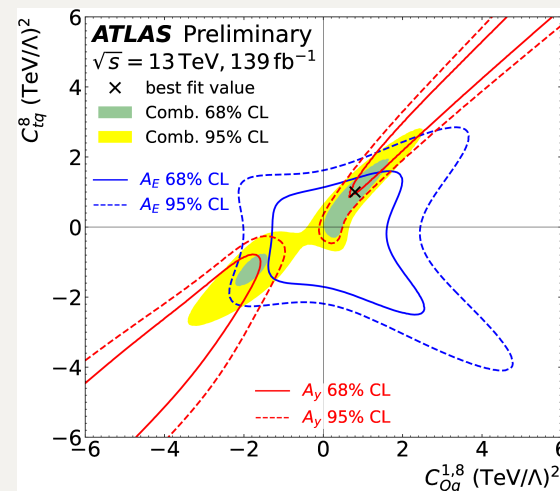
- $gg \rightarrow t\bar{t}$  production: charge-symmetric
  - $gq \rightarrow t\bar{t}q$  introduces asymmetry
  - BSM interactions can enhance asymmetry
- Asymmetry observables:  $A_y$  (single + di-lepton),

$A_E$  (single lepton + high  $p_T$  jet)

$$A_y = \frac{N(\Delta|y| > 0) - N(\Delta|y| < 0)}{N(\Delta|y| > 0) + N(\Delta|y| < 0)}, \text{ with } \Delta|y| = |y_t| - |y_{\bar{t}}|$$

$$A_E = \frac{\sigma_{E_A}}{\sigma_{E_S}} \text{ where } \sigma_{E,(A)S} \text{ is the charge-(a)symmetric cross-section}$$

- $A_y$  highly sensitive to SMEFT operators
  - Combination with  $A_E$  helps resolve  $c_{Qq}^{1,8}, C_{tq}^8$  flat direction



# Electroweak sector

## Going beyond $d = 6$

- Neutral triple gauge couplings (nTGC) and anomalous quartic gauge couplings (aQGC), appear at  $d = 8$ 
  - Not well constrained under current  $d = 6$  models
  - Couplings affect mostly vector boson scattering and  $VVV$  production

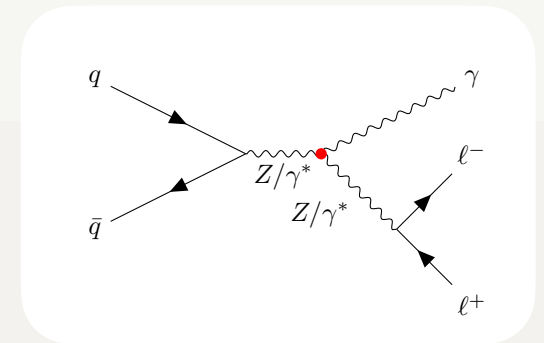
Violate lepton/baryon number conservation

$$\mathcal{L}_{\text{SMEFT}} = \mathcal{L}_{\text{SM}} + \sum_i \frac{c_i^{(5)}}{\Lambda} Q_i^{(5)} + \sum_i \frac{c_i^{(6)}}{\Lambda^2} Q_i^{(6)} + \sum_i \frac{c_i^{(7)}}{\Lambda^3} Q_i^{(7)} + \sum_i \frac{c_i^{(8)}}{\Lambda^4} Q_i^{(8)} + \dots$$

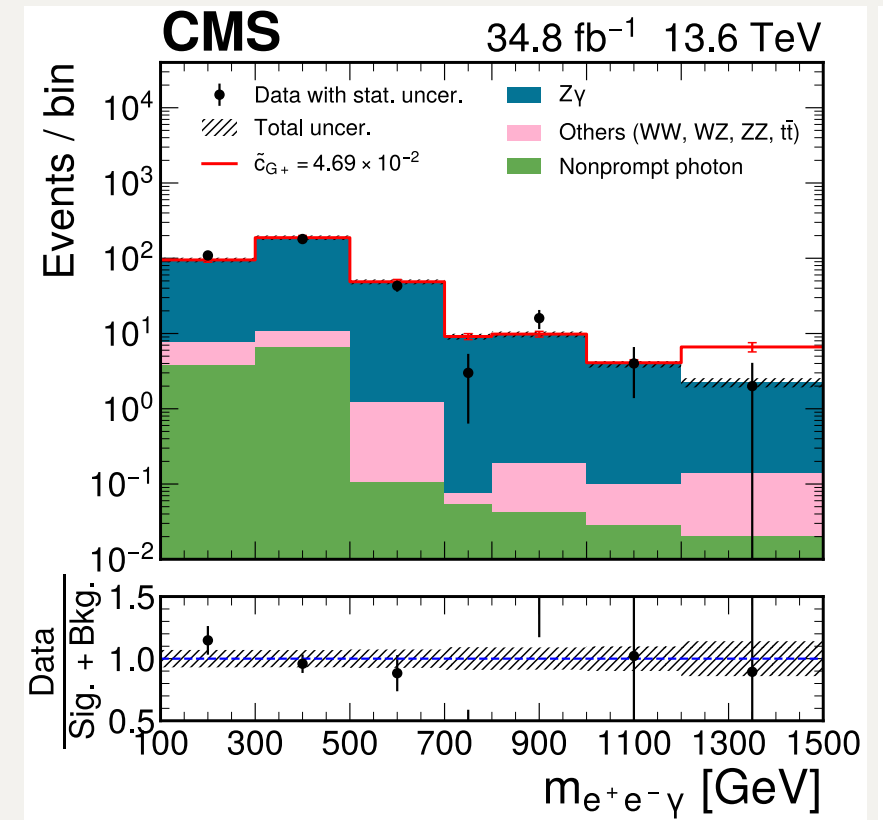
Highly constrained by available measurements

- GSPM and VPM models used to describe nTGC
- Éboli model used to describe aQGC

# Electroweak sector: nTGC



- nTGC constrained using  $Z\gamma$  measurement
  - One of most precise EW measurements at LHC (very clean signature)
  - High-mass  $Z\gamma \rightarrow$  sensitive to BSM effects
- Limits under two models:
  - VPM preserves only unbroken U(1) symmetry
  - GSPM maintains SU(2) x U(1) constraints
- **Limits on GSPM operators are weaker**

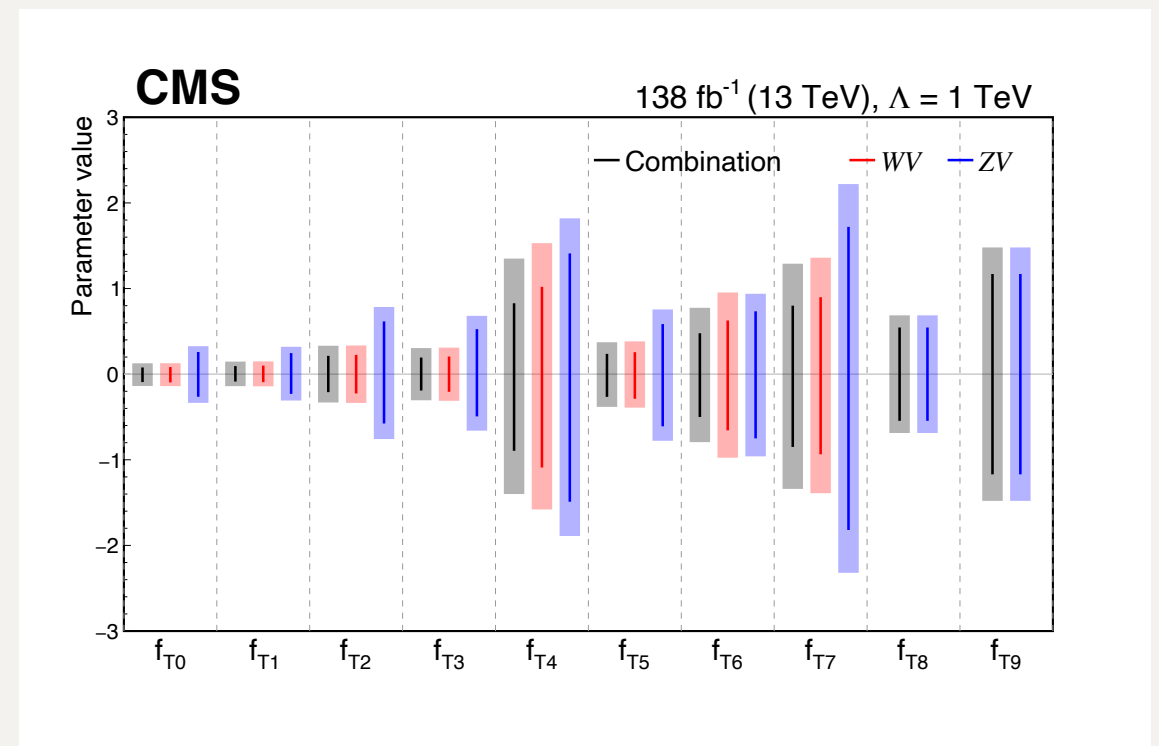
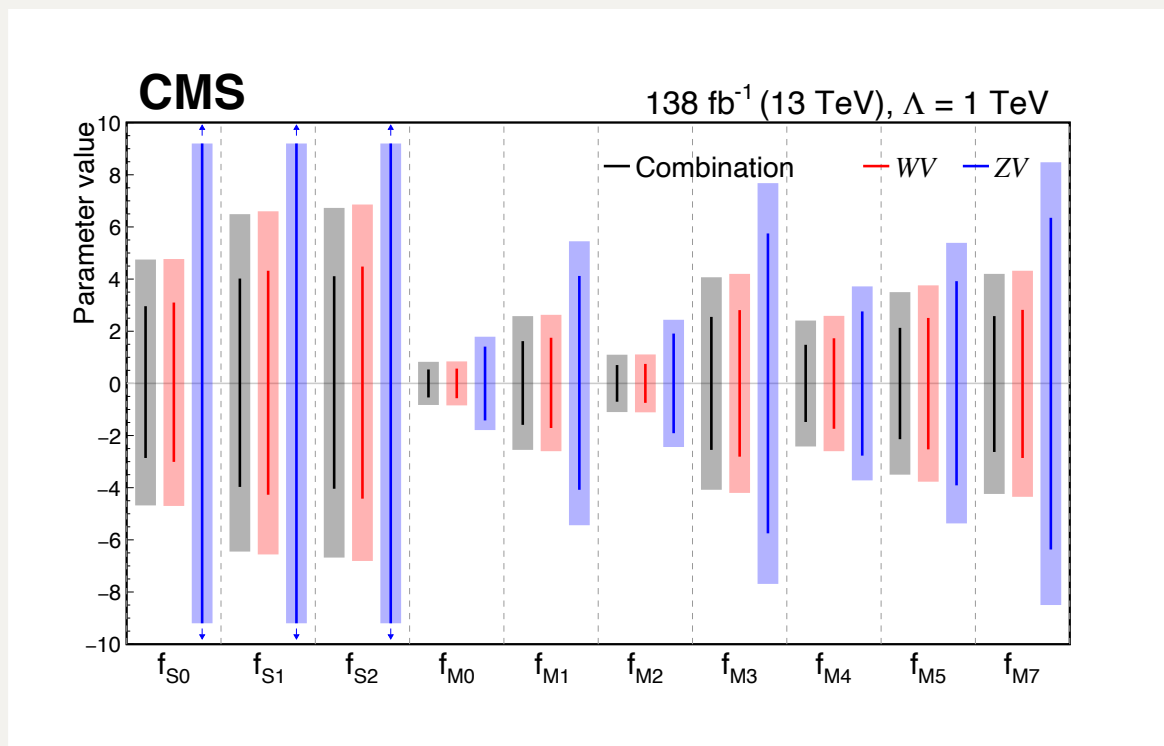
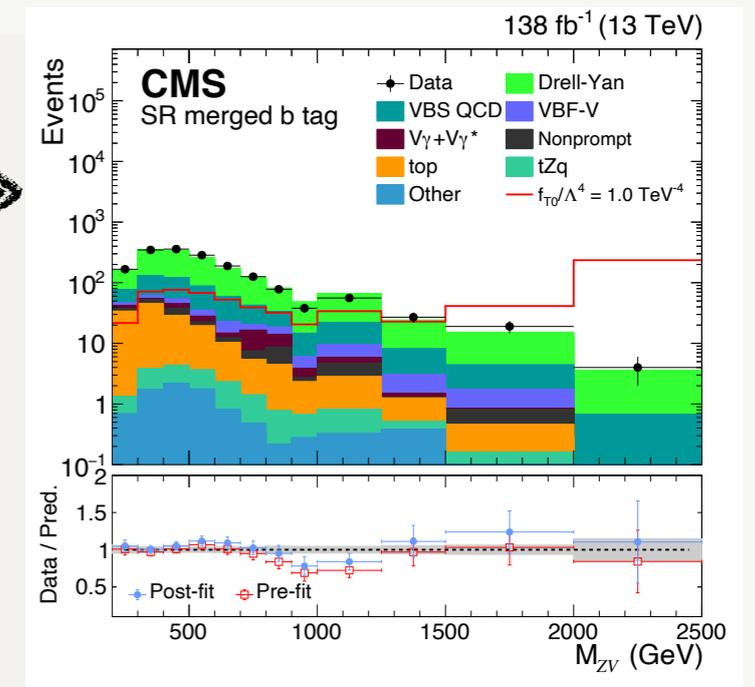


VPM  
GSPM

Limits	Expected		Observed	
	Lower	Upper	Lower	Upper
$h_4^Z$	$-1.01 \times 10^{-6}$	$1.01 \times 10^{-6}$	$-8.17 \times 10^{-7}$	$8.20 \times 10^{-7}$
$h_4^Z(\tilde{c}_{G+})$	$-4.60 \times 10^{-5}$	$4.64 \times 10^{-5}$	$-3.71 \times 10^{-5}$	$3.70 \times 10^{-5}$

# Electroweak sector: aQGC

- Input measurements:
  - $WW, WZ, ZZ$  in lepton+jets final states
- Fit to  $M_{VV}$ , found to be sensitive to aQGC effects
- **Small impact from clipping unitarisation scheme reported**
  - aQGC zeroed above certain energy to avoid unitarity violation



# Electroweak sector: aQGC

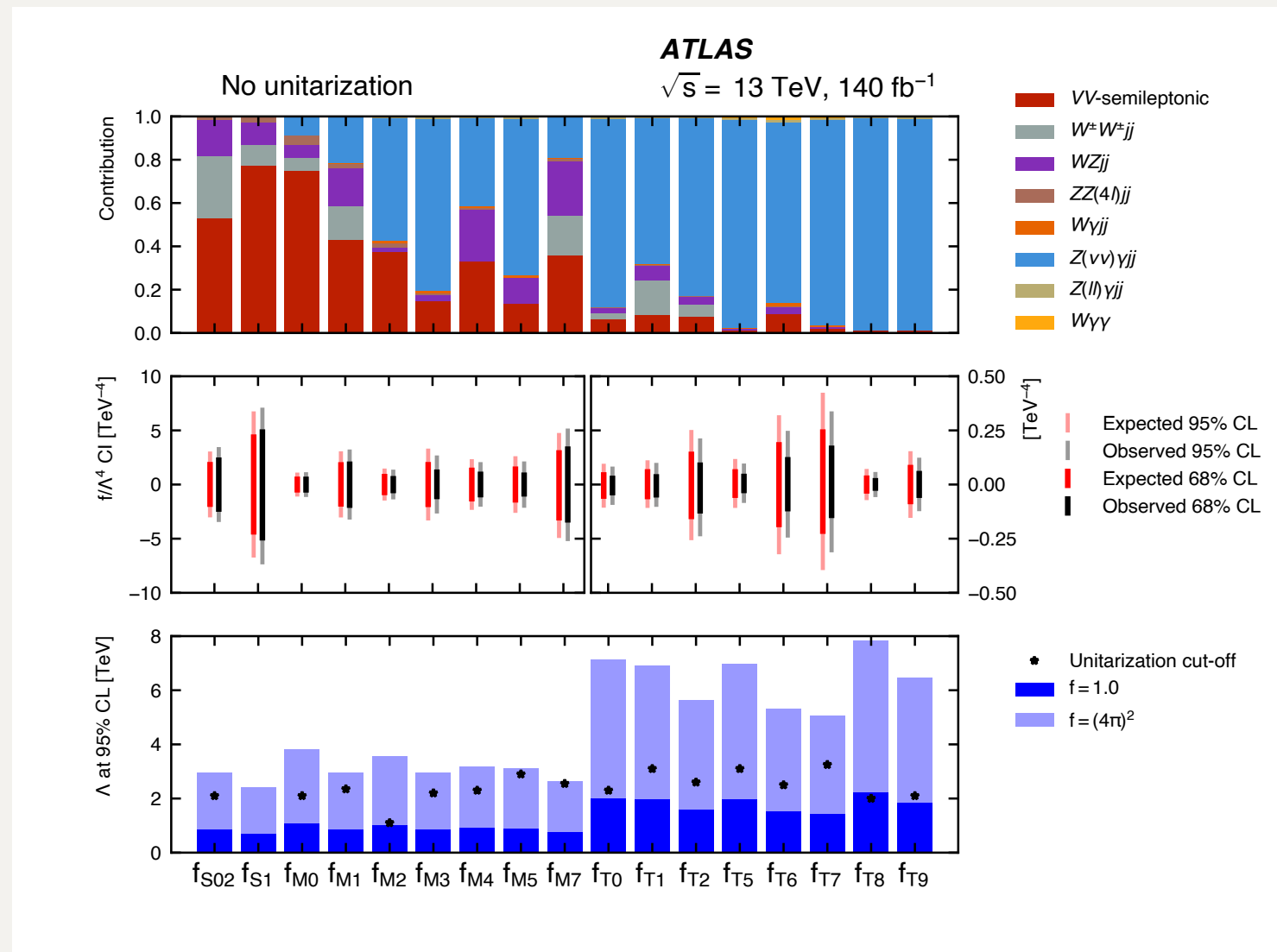
NEW

- Combination + re-interpretation of 8 input measurements
  - Differential distributions + inclusive cross-sections

- **Reports larger impact from clipping**

- 1 order of magnitude weaker constraints for 1.5 TeV clipping

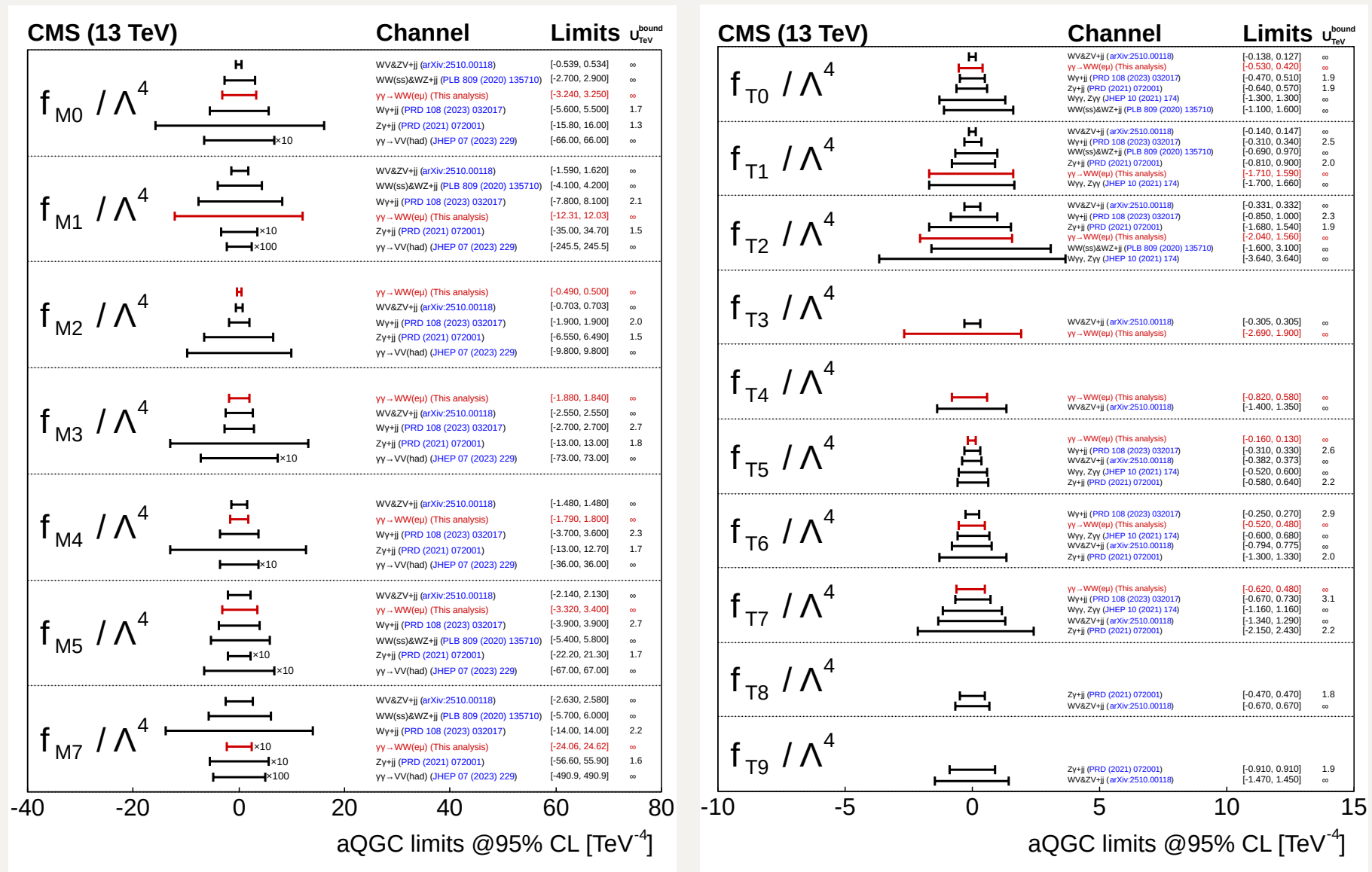
- Results driven by  $Z\gamma + 2j \rightarrow \nu\bar{\nu}\gamma + 2j$  and  $VV + 2j \rightarrow (\ell\ell, \ell\nu, \nu\nu)jj + 2j$



# Electroweak sector: $\gamma\gamma \rightarrow WW$

- Photon-fusion production mediated by (triple and) quartic gauge couplings
  - In SM, destructive interference preserves unitarity  $\rightarrow$  could be disturbed by BSM effects

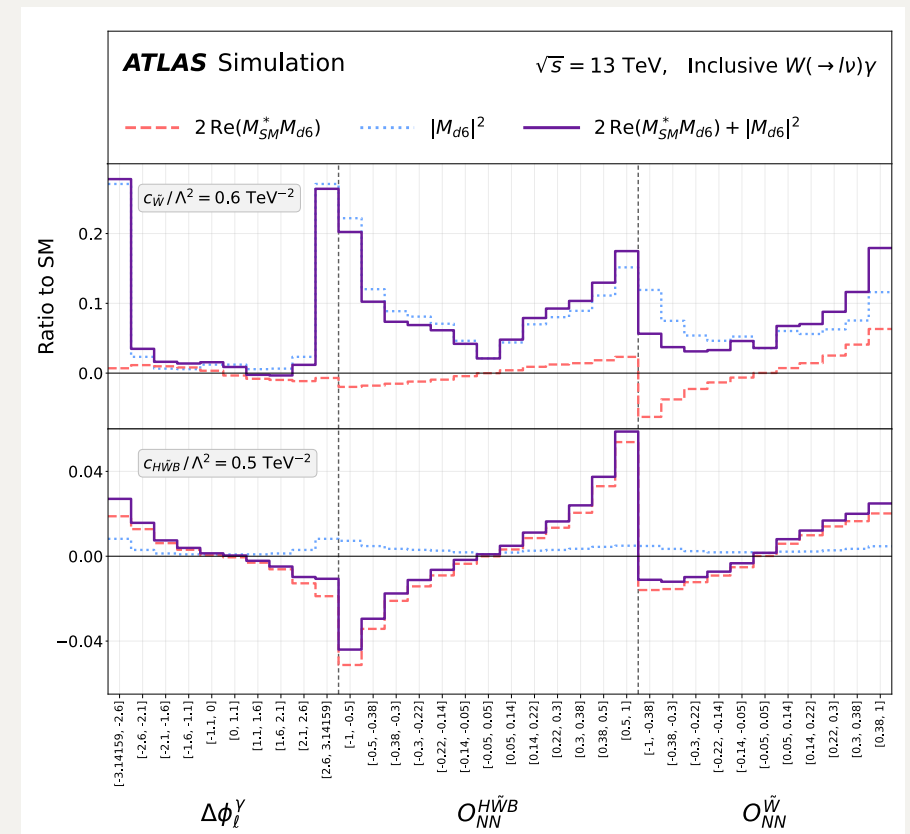
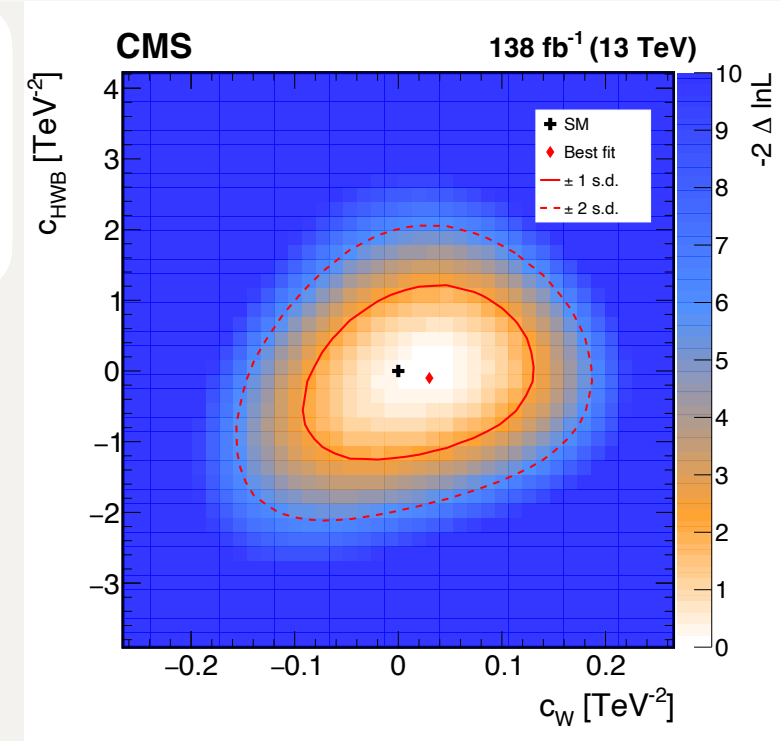
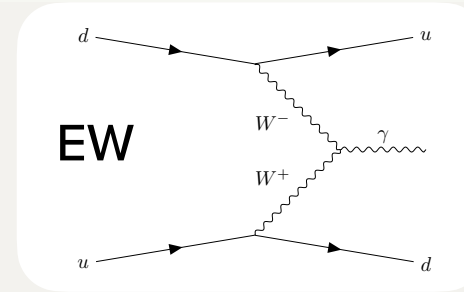
Sensitivity competitive with other EW results for many operators



# Electroweak sector: $\gamma$

Back to  $d = 6$

- VBF production sensitive to BSM interactions in  $WW\gamma$  vertex ( $c_W, c_{HWB}$ )
  - Separate EW and QCD  $\gamma + 2j$  using kinematic information from the  $\gamma$  and the  $j$ s
    - **DNN for SM/BSM separation**
- $W\gamma$  production also sensitive to BSM interactions in  $WW\gamma$  vertex ( $c_W, c_{HWB}, c_{\tilde{W}}, c_{H\tilde{W}B}$ )
  - CP sensitivity from  $\Delta\phi_{\ell\gamma}$  and NN-based optimal observable
    - Sensitivity to  $c_{H\tilde{W}B}$  significantly improved wrt other measurements:  $[-0.60, 0.13]$  at 95% CL



# Global fits

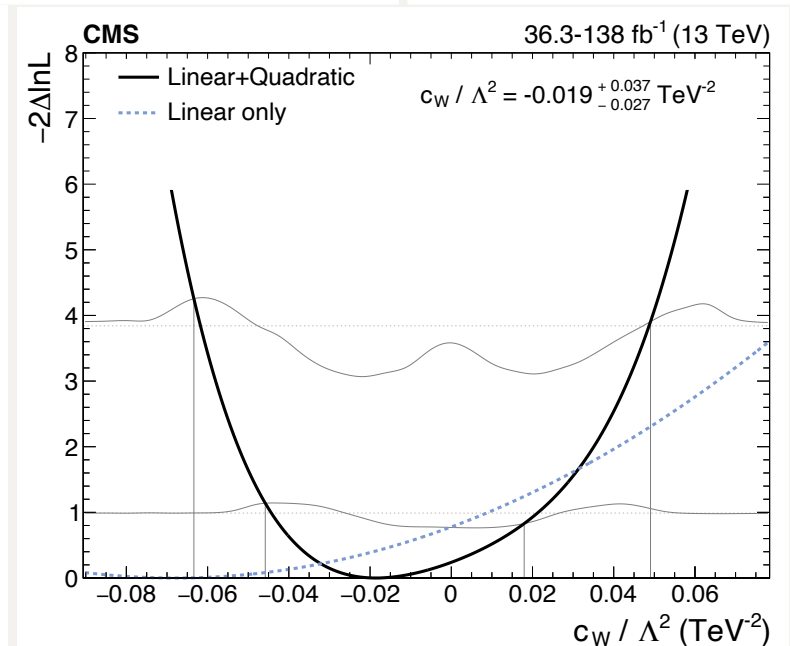
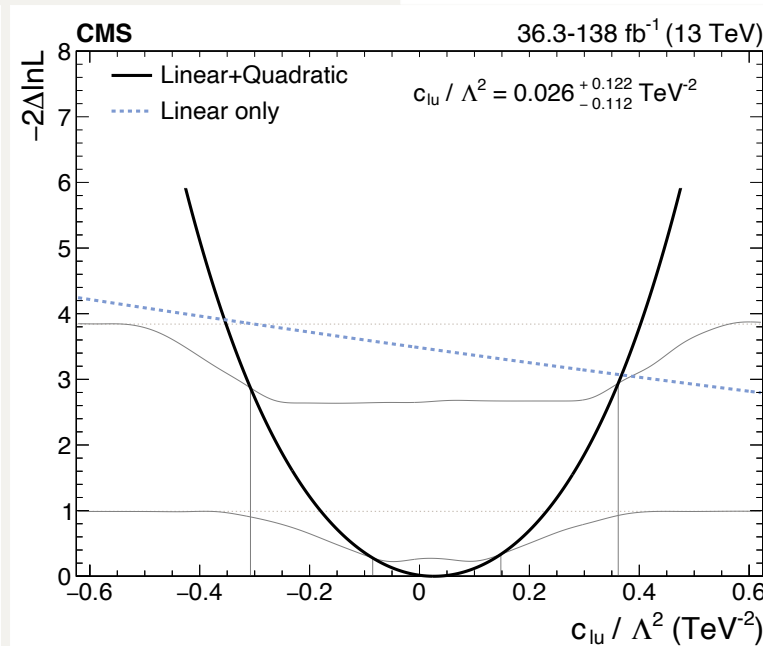
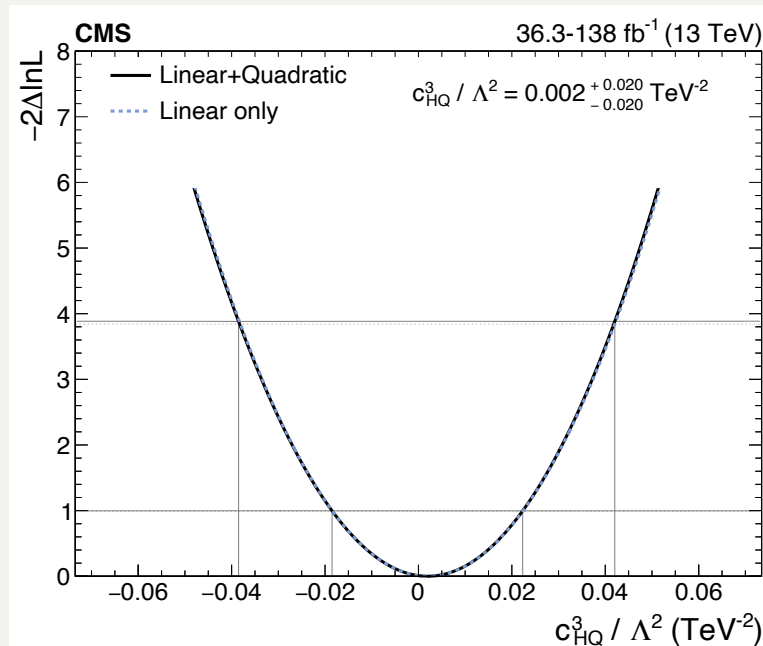
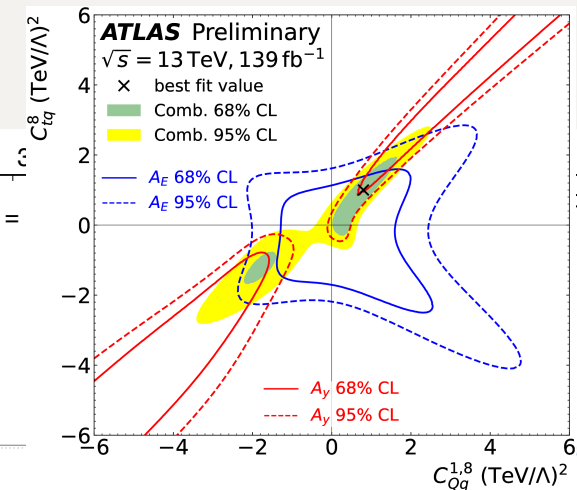
- CP-conserving operators only
  - Top-flavour symmetry scheme
- Generally, BSM effects only considered for signal processes
- Acceptance effects taken into account for 4-body decays
- **One-at-a-time fits (64 operators) + multi-coefficient constraints (PCA, 42 EVs)**  
**+ results with simplified model using covariance matrix**

Analysis	Type of measurement	Observables used	Experimental likelihood
$H \rightarrow \gamma\gamma$	Differential cross sections	STXS bins [54]	✓
$W\gamma$	Fiducial differential cross sections	$p_T^\gamma \times  \phi_f $ [33]	✓
$Z \rightarrow \nu\nu$	Fiducial differential cross sections	$p_T^Z$	✓
WW	Fiducial differential cross sections	$m_{\ell\ell}$	✓
$t\bar{t}$	Fiducial differential cross sections	$m_{t\bar{t}}$	×
$t(\bar{t})X$	Direct EFT	Yields in regions of interest	✓
Inclusive jet	Fiducial differential cross sections	$p_T^{\text{jet}} \times  y^{\text{jet}} $	×
EWPO	Pseudo-observables	$\Gamma_Z, \sigma_{\text{had}}^0, R_\ell, R_c, R_b, A_{\text{FB}}^{0,\ell}, A_{\text{FB}}^{0,c}, A_{\text{FB}}^{0,b}$ [36]	×



# Conclusion + general comments (1/2)

- Many results in (very) non-Gaussian regime
  - Tests done by CMS in global EFT fit
  - Can affect the 95% CLs quite a bit!
    - **Larger effect when quad terms are important**
    - **Generally LH steep around 95% line so (luckily) results relatively stable**



# Conclusion + general comments (2/2)

- Many new EFT results using Run 2 data + first results with Run 3 data
- EFT fits benefit from **combinations** (esp. to resolve flat directions)
  - Important that input analyses be orthogonal → not always the case!
  - Addressed by cutting away overlap in phase-space/events, bootstrapping
- **Interesting/new techniques** to improve measurements
  - PCA to reduce correlations between parameters
  - ADNN to reduce model dependence
- Non-trivial impact of missing  $d = 8$  terms / linear vs lin+quad parametrisations, clipping schemes, ... but very analysis/result-dependent
- Overall, results tend to be limited by available statistics → Run 3 data very useful

Backup/other

# Higgs sector

- Look for BSM effects in  $H$  interactions (production and decay)
- Mostly measurements reinterpreted within SMEFT
  - CP, (fiducial) cross-sections, STXS, ...
- Usually parametrised as “expansions” of the SM signal strength
  - Taylor expansion used to retain linear-only terms
  - Focus on  $d = 6$

$$\mu_{j,\text{prod}}(\vec{c}) = 1 + \frac{\sigma_j^{\text{int}}}{\sigma_j^{\text{SM}}} + \frac{\sigma_j^{\text{BSM}}}{\sigma_j^{\text{SM}}},$$

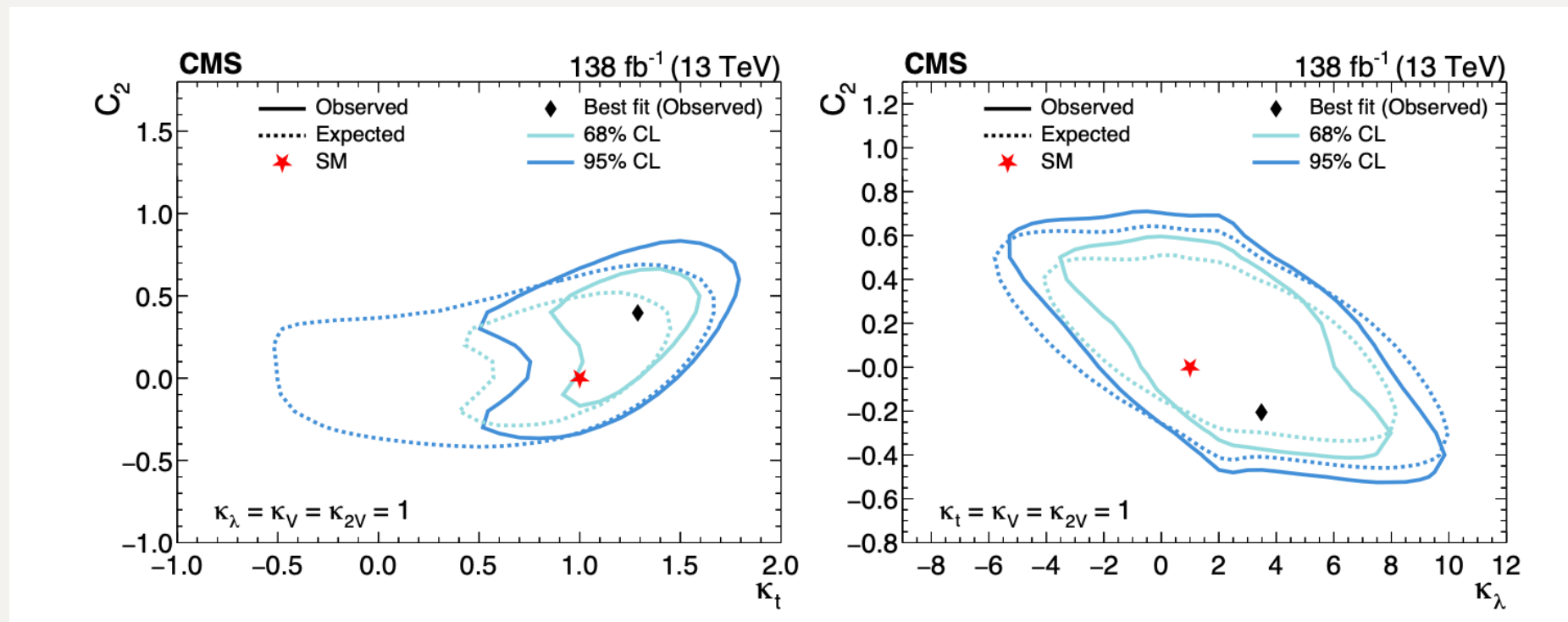
$$\mu_{j,\text{decay}}(\vec{c}) = \frac{\Gamma_{\text{SMEFT}}^{\text{H} \rightarrow \text{WW}} / \Gamma_{\text{SM}}^{\text{H} \rightarrow \text{WW}}}{\Gamma_{\text{SMEFT}}^{\text{H}} / \Gamma_{\text{SM}}^{\text{H}}} = \frac{1 + \sum_k A_k^{j,\text{H} \rightarrow \text{WW}} c_k + \sum_{kl} B_{kl}^{j,\text{H} \rightarrow \text{WW}} c_k c_l}{1 + \sum_k A_k^{\text{H}} c_k + \sum_{kl} B_{kl}^{\text{H}} c_k c_l}.$$

$$\mu_j(\vec{c}) = \frac{\sigma_j^{\text{SMEFT}}}{\sigma_j^{\text{SM}}} \frac{\mathcal{B}_{j,\text{SMEFT}}^{\text{H} \rightarrow \text{WW}}}{\mathcal{B}_{j,\text{SM}}^{\text{H} \rightarrow \text{WW}}} = \mu_{j,\text{prod}}(\vec{c}) \mu_{j,\text{decay}}(\vec{c}),$$

# Higgs sector: combinations

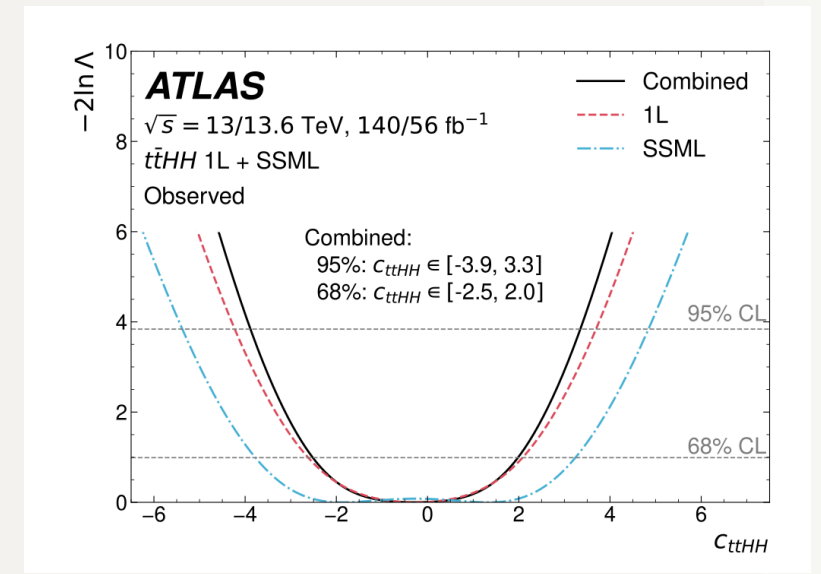
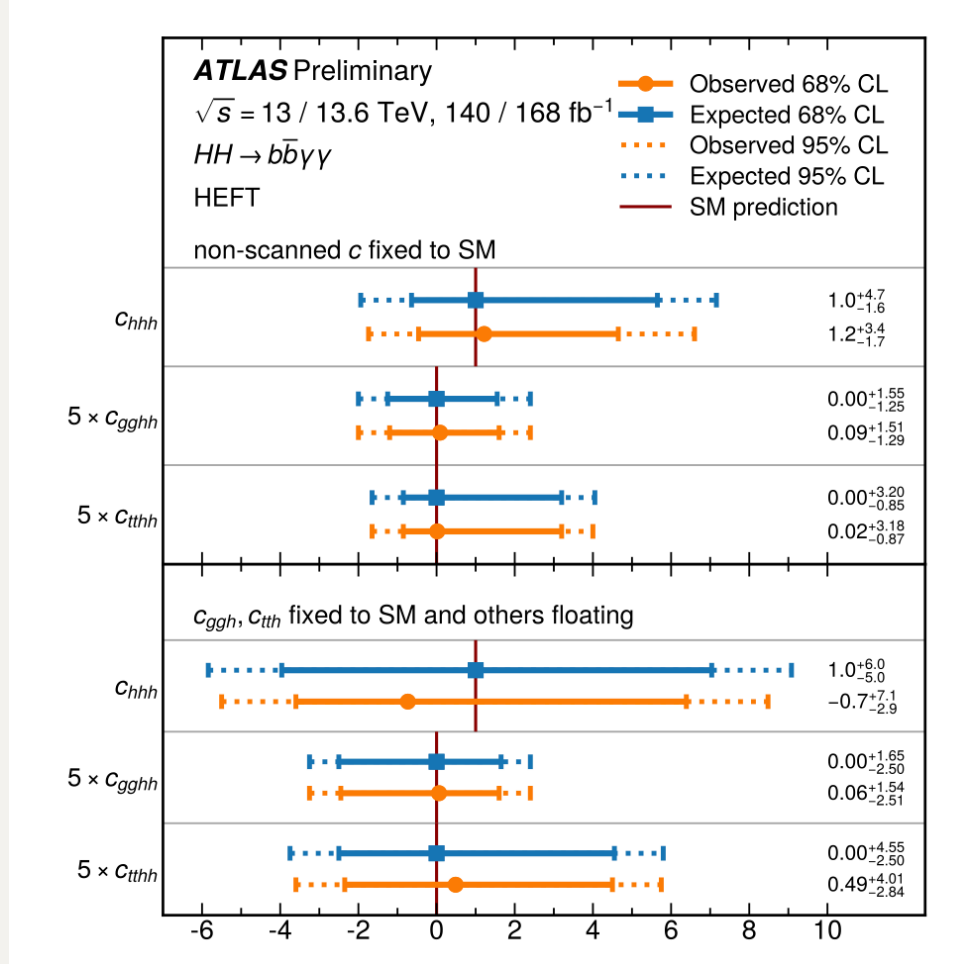
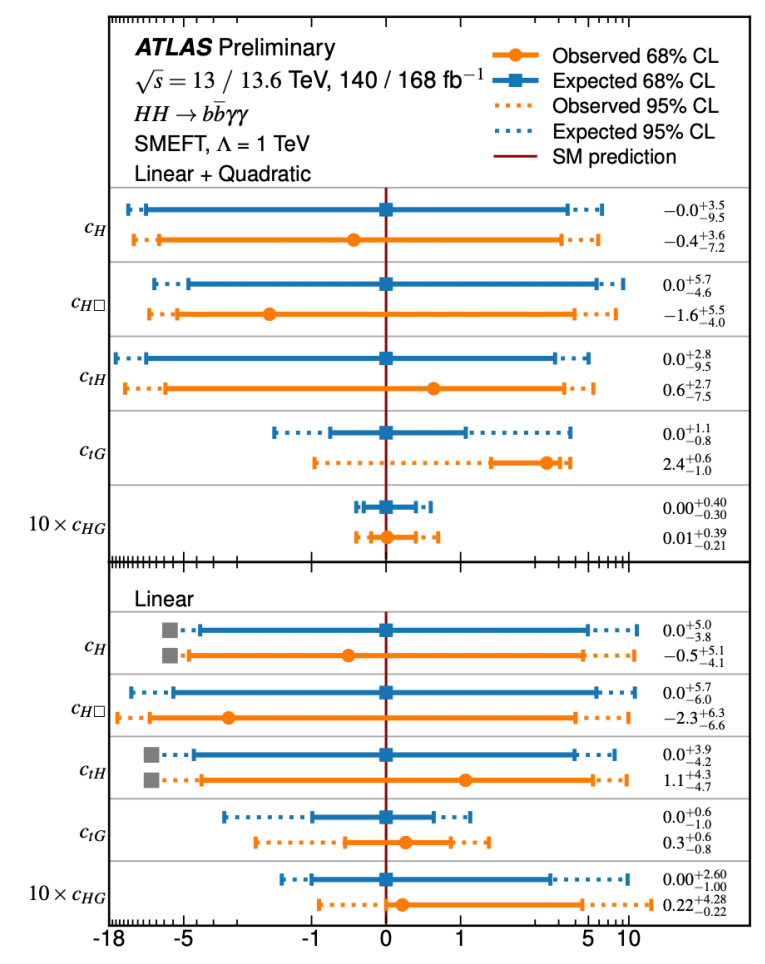
Oct 2025

- 3 BSM couplings considered:  $c_2, c_g, c_{2g}$  ( $ttHH, ggH, ggHH$  vertices)
  - Considering also  $\kappa_t, \kappa_{2V}, \kappa_V, \kappa_\lambda$
  - Only  $ggHH$  production floated,  $VBFHH$  set to SM
  - Samples re-weighted to account for BSM effects
    - Parametrised in  $m_{HH}$  and  $\Delta\phi_{HH}$
- Input measurements:  $b\bar{b}\gamma\gamma, b\bar{b}b\bar{b}, b\bar{b}\tau\tau, b\bar{b}WW, ML, WW\gamma\gamma, \tau\tau\gamma\gamma$ 
  - 95% CL exclusion on  $c_2$  is  $-0.29$  to  $0.63$  ( $-0.27$  to  $0.56$  expected)



# Higgs sector: $HH$ production

- SMEFT and HEFT frameworks used to model EFT
  - HEFT decouples the Higgs boson from the EW gauge structure
  - Interpretations for  $ggHH$  and VBF $HH$ ,  $HH \rightarrow b\bar{b}\gamma\gamma$ 
    - 95% CL exclusion on  $c_{ttHH}$  is -0.33 to 0.80 (-0.72 to 1.15 expected)
    - Complementary bounds from  $t\bar{t}HH$  on  $c_{tthh}$



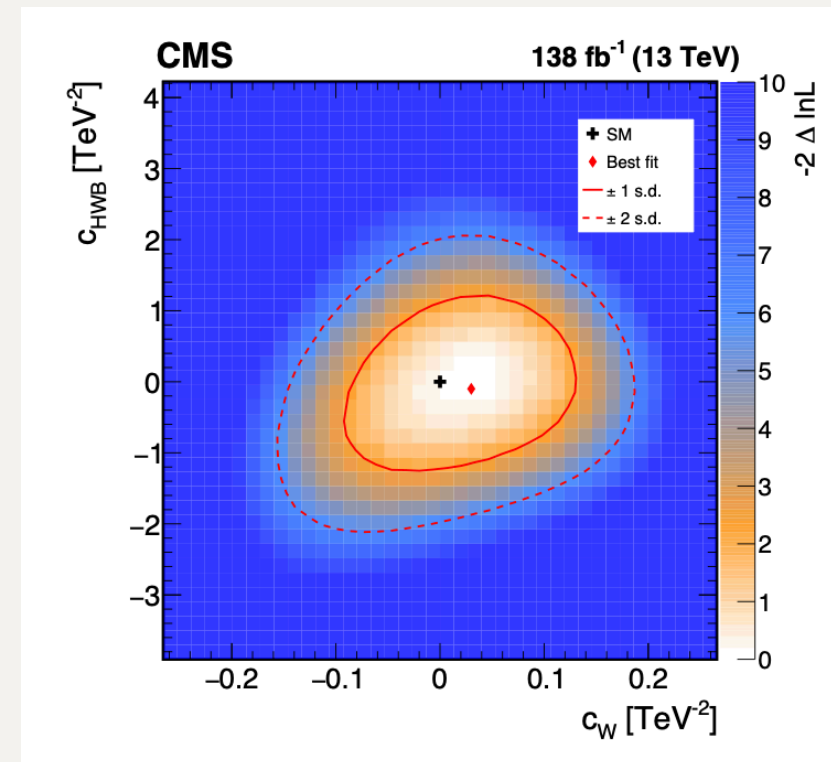
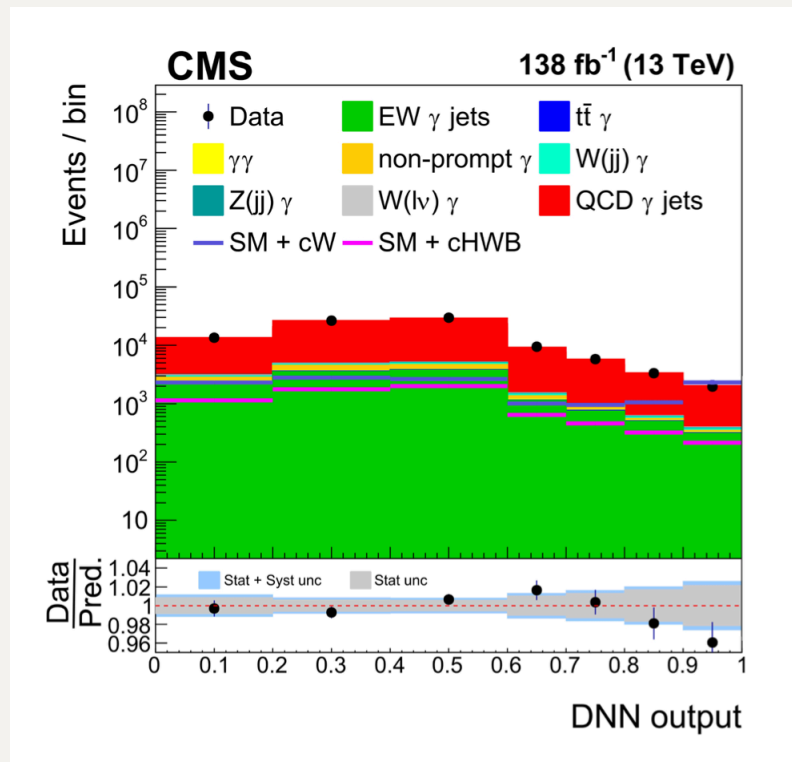
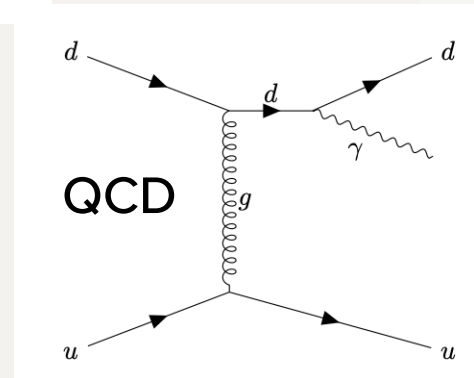
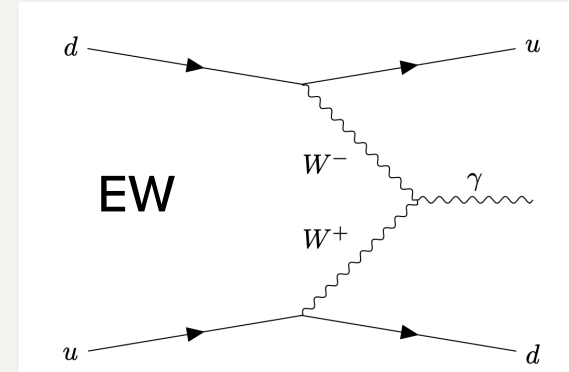
# Top sector

- Focusing mostly on differential measurements to constrain Wilson coefficients
  - Analyses typically target subset of relevant operators
  - Production and decay processes are sensitive to different operators
  - Focus on  $d = 6$
- Higgs results mainly dominated by statistical uncertainties
  - In top sector, systematic uncertainties play a larger role

# Electroweak sector: $\gamma + 2j$

Nov 2025

- VBF production sensitive to triboson interactions
  - Analysis aims to separate EW and QCD  $\gamma + 2j$  using kinematic information from the  $\gamma$  and the  $js$
  - Sensitive to BSM interactions in the  $WW\gamma$  vertex ( $c_W, c_{HWB}$ )
    - DNN trained to distinguish pure SM from (linear + quad) BSM terms  $\rightarrow$  DNN can handle negative weights fairly well



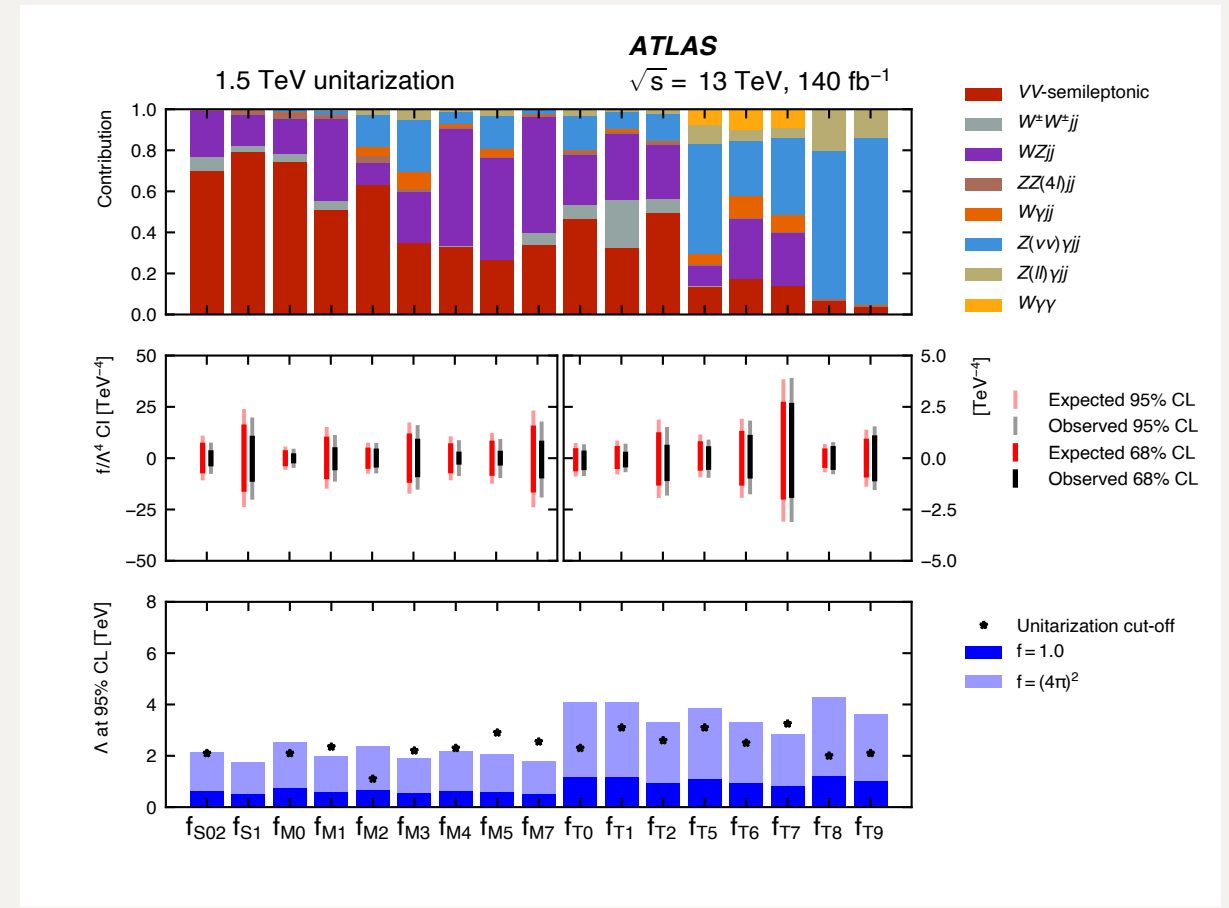
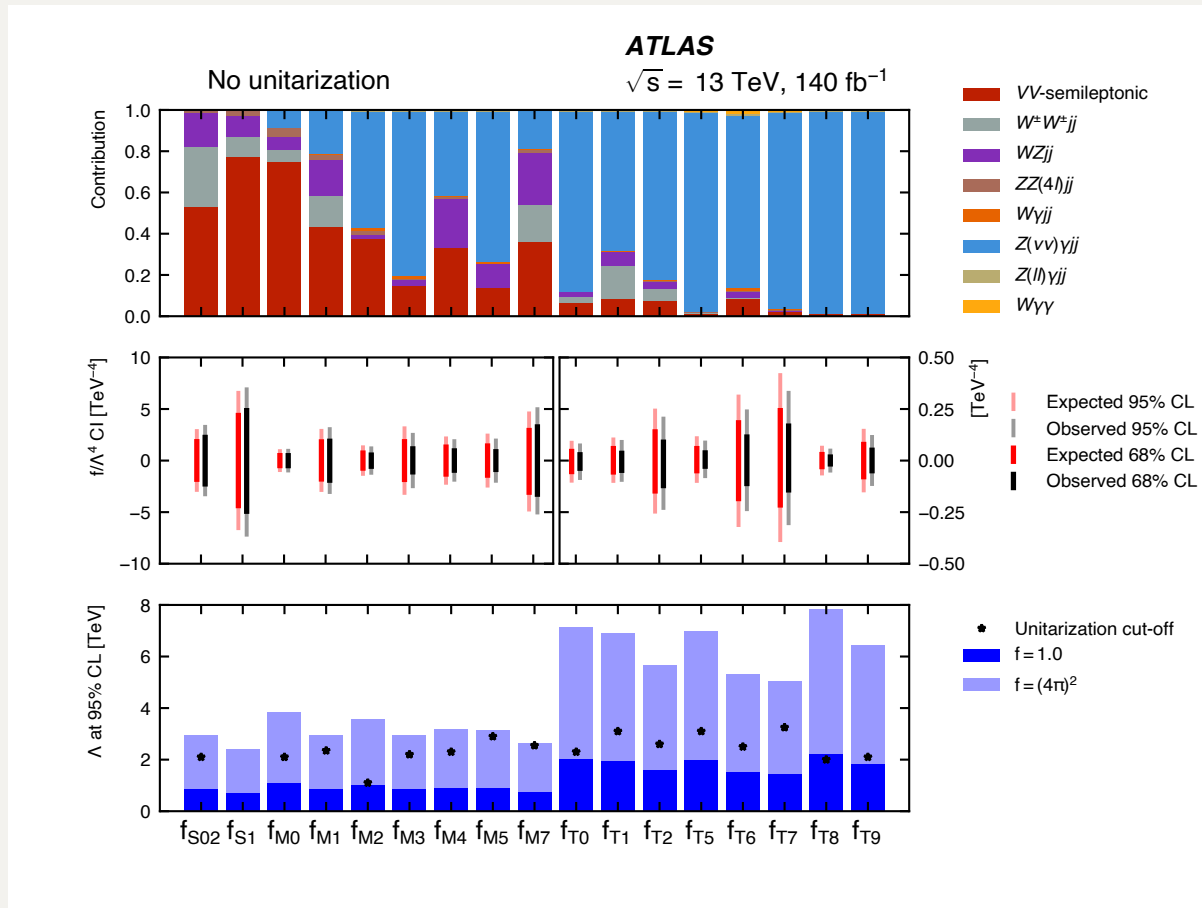
# Electroweak sector: aQGC

Oct 2025

- Input measurements:
  - $WWW, WWZ, WZZ, ZZZ$  using large-R jet  $V$  taggers
- $d = 6 + 8$  operators (Warsaw + Éboli bases, 12+20 operators)
- Fit to  $S_T$  (scalar sum of  $p_T$  of leptons + jets) to approximate  $m_{VVV}$

# Electroweak sector: aQGC

NEW



# VVV: CMS-PAS-SMP-24-017

Table 5: Summary of the 95% CL bounds on the dim-6 Wilson coefficients. We consider the case of a single varying Wilson coefficient (“Freeze other WCs”) as well as the case when the other Wilson coefficients are profiled (“Profile other WCs”). The Wilson coefficients are ordered by increasing confidence interval width.

Wilson coefficient	Freeze other WCs		Profile other WCs	
	95% CL bounds [ TeV <sup>-2</sup> ]		95% CL bounds [ TeV <sup>-2</sup> ]	
	Observed	Expected	Observed	Expected
$c_W / \Lambda^2$	[-0.13, 0.12]	[-0.12, 0.12]	[-0.11, 0.11]	[-0.13, 0.13]
$c_{Hq3} / \Lambda^2$	[-0.24, 0.21]	[-0.23, 0.20]	[-0.40, 0.29]	[-0.30, 0.26]
$c_{Hq1} / \Lambda^2$	[-0.34, 0.34]	[-0.32, 0.32]	[-0.39, 0.40]	[-0.35, 0.34]
$c_{Hu} / \Lambda^2$	[-0.60, 0.59]	[-0.61, 0.59]	[-0.84, 0.67]	[-0.75, 0.73]
$c_{Hd} / \Lambda^2$	[-0.79, 0.79]	[-0.79, 0.79]	[-0.75, 0.93]	[-0.87, 0.89]
$c_{HW} / \Lambda^2$	[-1.60, 1.55]	[-1.63, 1.55]	[-2.0, 3.0]	[-2.1, 2.4]
$c_{HWB} / \Lambda^2$	[-5.2, 5.0]	[-5.5, 5.2]	[-7.2, 9.2]	[-7.8, 7.7]
$c_{H\ell3} / \Lambda^2$	[-4, 1] $\cup$ [9, 17]	[-3, 15]	[-16, 29]	[-12, 26]
$c_{HB} / \Lambda^2$	[-11, 11]	[-12, 12]	[-8.3, 8.6]	[-13, 13]
$c_{\ell\ell1} / \Lambda^2$	[-32, -13] $\cup$ [-9, 10]	[-30, 7]	[-48, 26]	[-44, 22]
$c_{H\Box} / \Lambda^2$	[-76, 69]	[-69, 61]	[-74, 75]	[-61, 60]
$c_{HDD} / \Lambda^2$	[-114, 71]	[-108, 68]	[-116, 67]	[-125, 74]

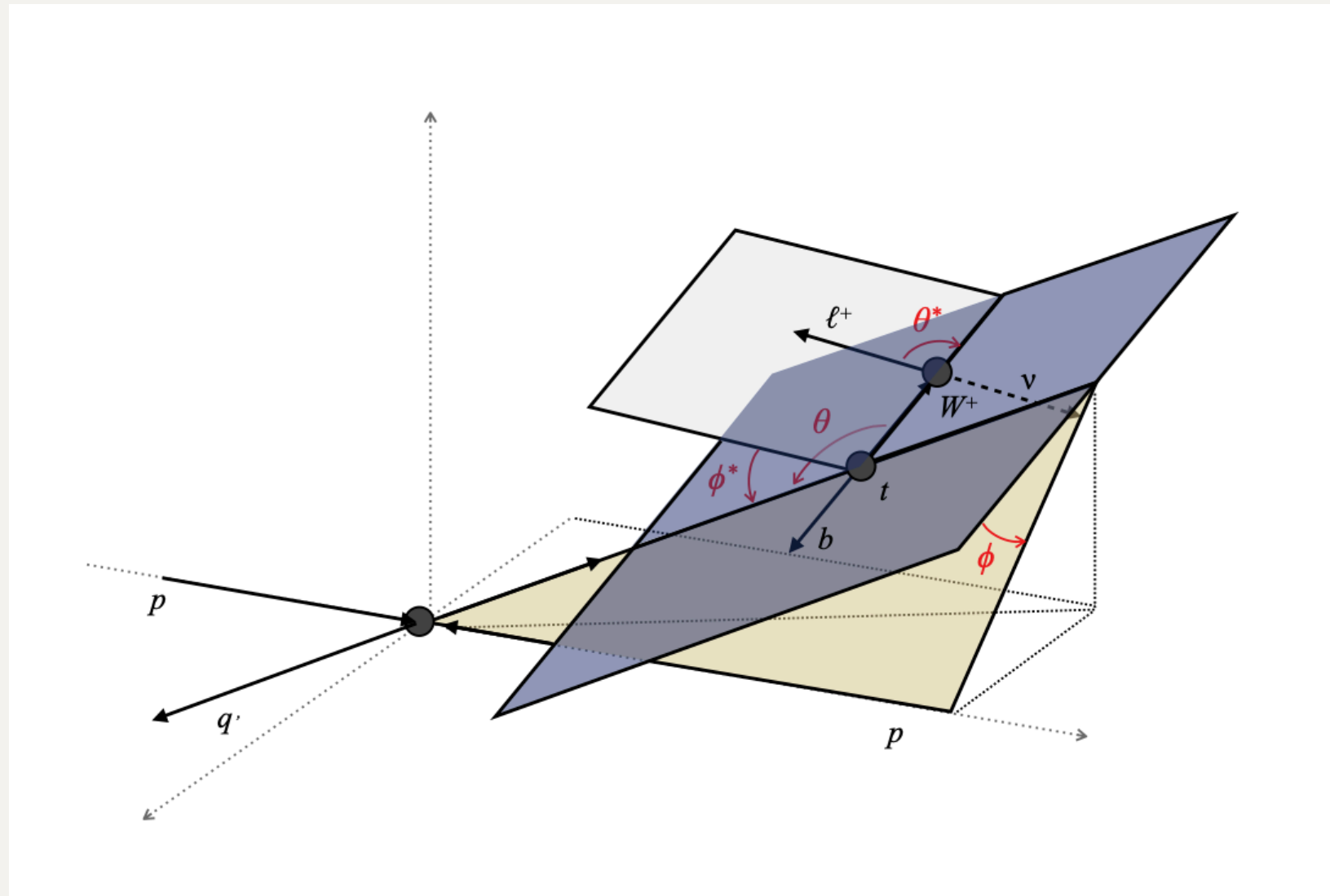
Table 6: Summary of the 95% CL bounds and measurements on the dim-8 Wilson coefficients, when considering a single varying Wilson coefficient at a time. The Wilson coefficients are ordered by increasing confidence interval width.

Wilson coefficient	95% CL bounds [ TeV <sup>-4</sup> ]		Measurement [ TeV <sup>-4</sup> ]
	Observed	Expected	Observed
$f_{T,0}/\Lambda^4$	[-0.57, 0.63]	[-0.48, 0.54]	$-0.05^{+0.34}_{-0.28}$
$f_{T,1}/\Lambda^4$	[-0.63, 0.70]	[-0.54, 0.62]	$0.05^{+0.26}_{-0.41}$
$f_{T,3}/\Lambda^4$	[-1.22, 1.32]	[-1.04, 1.18]	$0.10^{+0.48}_{-0.82}$
$f_{T,2}/\Lambda^4$	[-1.29, 1.39]	[-1.10, 1.24]	$0.10^{+0.50}_{-0.85}$
$f_{M,0}/\Lambda^4$	[-3.8, 4.0]	[-2.8, 3.2]	$-0.4^{+2.9}_{-1.8}$
$f_{T,5}/\Lambda^4$	[-4.0, 3.9]	[-3.1, 3.0]	$0.0^{+2.6}_{-2.7}$
$f_{T,6}/\Lambda^4$	[-4.9, 4.8]	[-3.8, 3.7]	$0.0^{+3.2}_{-3.3}$
$f_{M,1}/\Lambda^4$	[-6.7, 6.4]	[-5.0, 5.1]	$-1.0^{+4.7}_{-3.0}$
$f_{T,4}/\Lambda^4$	[-9.2, 9.0]	[-7.1, 7.0]	$0.0^{+6.0}_{-6.0}$
$f_{T,7}/\Lambda^4$	[-10, 10]	[-8, 8]	$0.1^{+6.8}_{-7.1}$
$f_{M,7}/\Lambda^4$	[-10, 11]	[-8, 9]	$-1.0^{+6.7}_{-4.4}$
$f_{M,5}/\Lambda^4$	[-11, 11]	[-9, 9]	$0.0^{+7.3}_{-7.0}$
$f_{T,8}/\Lambda^4$	[-11, 12]	[-7, 7]	$5^{+3}_{-13}$
$f_{M,4}/\Lambda^4$	[-13, 13]	[-11, 11]	$0.0^{+8.7}_{-8.4}$
$f_{M,2}/\Lambda^4$	[-14, 14]	[-11, 11]	$0.0^{+9.7}_{-9.7}$
$f_{T,9}/\Lambda^4$	[-22, 23]	[-14, 14]	$11^{+5}_{-27}$
$f_{M,3}/\Lambda^4$	[-23, 23]	[-18, 18]	$0^{+16}_{-15}$
$f_{S,1}/\Lambda^4$	[-26, 26]	[-24, 25]	$-2^{+16}_{-13}$
$f_{S,0}/\Lambda^4$	[-38, 38]	[-35, 35]	$-2^{+22}_{-20}$
$f_{S,2}/\Lambda^4$	[-38, 39]	[-36, 36]	$-2^{+22}_{-20}$

# CMS H combination

Input analysis	Decay channels targeted	Production targeted	Signal granularity	References
$H \rightarrow \gamma\gamma$	$\gamma\gamma$	ggH, $(NJ, p_T^H, m_{jj})$ bins VBF, $(p_T^H, m_{jj}, p_T^{Hjj})$ bins VH hadronic WH leptonic, $p_T^V$ bins ZH leptonic ttH, $p_T^H$ bins tH	STXS stage 1.2	[42]
$H \rightarrow ZZ \rightarrow 4\ell$	$4\mu, 2e2\mu, 4e$	ggH, $(NJ, p_T^H, m_{jj})$ bins VBF, $(NJ, p_T^H, m_{jj}, p_T^{Hjj})$ bins VH hadronic VH leptonic, $p_T^V$ bins ttH	STXS stage 1.2	[43]
$H \rightarrow WW \rightarrow \ell\nu\ell\nu$	$e\mu/\mu e, ee+\mu\mu, e\mu+jj$ $3\ell, 4\ell$	ggH, $(NJ, p_T^H)$ bins VBF-like $(p_T^H, m_{jj})$ bins VH hadronic WH leptonic, $p_T^V$ bins ZH leptonic, $p_T^V$ bins	STXS stage 1.2	[44]
$H \rightarrow \tau\tau$	$e\mu, e\tau_h, \mu\tau_h, \tau_h\tau_h$ $e\tau_h+2\ell, \mu\tau_h+\ell/2\ell, \tau_h\tau_h+\ell/2\ell$	ggH, $(NJ, p_T^H, m_{jj})$ bins VBF, $(NJ, p_T^H, m_{jj})$ bins WH leptonic, $p_T^V$ bins ZH leptonic, $p_T^V$ bins	Inclusive production processes or STXS stage 1.2	[45]
$H \rightarrow bb$ boosted	bb	ggH, high- $p_T^H$ bins VBF, high- $p_T^H$ bins	Inclusive production processes or STXS stage 1.2	[27]
VBF ( $H \rightarrow bb$ )	bb	VBF	Inclusive production processes	[26]
VH ( $H \rightarrow bb$ )	bb	WH leptonic, $p_T^V$ bins ZH leptonic, $p_T^V$ bins	STXS stage 1.2	[30]
t(t)H ( $H \rightarrow bb$ )	bb	ttH, $p_T^H$ bins tH	Inclusive production processes or STXS stage 1.2	[31]
t(t)H ( $H \rightarrow$ leptons)	$2\ell(\text{same charge}), 3\ell, 4\ell$ $1\ell+2\tau_h, 2\ell(\text{same charge})+1\tau_h, 3\ell+1\tau_h$	ttH, tH	STXS stage 1.2	[46]
$H \rightarrow \mu\mu$	$\mu\mu$	ggH, VBF, VH, ttH	Inclusive production processes	[47]
$H \rightarrow Z\gamma \rightarrow \ell\ell\gamma$	$\ell\ell\gamma$	ggH, VBF	Inclusive production processes	[48]
$H \rightarrow$ inv	Large $p_T^{\text{miss}}$	Monojet VBF VH leptonic VH/ttH hadronic	Inclusive production processes	[29, 49–51]
Off-shell ( $H \rightarrow ZZ \rightarrow 4\ell$ )	$4\ell$	Off-shell	Off-shell contributions (cf. Eq. (17))	[28]

# 4 angles (single top)



# $t\bar{t}$ charge asymmetry: $A_y$

In  $t\bar{t}$  production, the charge asymmetry effect can be measured as central-forward rapidity asymmetry ( $A_Y$ ) [4, 5], which is expressed via the rapidity of the top quark ( $y_t$ ) and top antiquark ( $y_{\bar{t}}$ ) as follows:

$$A_Y = \frac{N(\Delta|y| > 0) - N(\Delta|y| < 0)}{N(\Delta|y| > 0) + N(\Delta|y| < 0)}, \quad (1)$$

where  $\Delta|y| = |y_t| - |y_{\bar{t}}|$ . The sign of  $\Delta|y|$  provides the information about the direction of flight of the top quark. In  $q\bar{q}$  annihilation, larger absolute rapidity values are expected from a particle which emerges in the direction of the incoming quark, as this valence quark carries a larger fraction of the proton momentum than the interacting sea antiquark.

# $t\bar{t}$ charge asymmetry: $A_E$

The charge asymmetry can also be tested at LO in QCD using the top-quark pair production associated with a hard jet ( $t\bar{t}j$ ), which contributes to the inclusive  $t\bar{t}$  production at NLO in QCD. In  $t\bar{t}j$  production, taking into account the relation between the particles' four momenta in the final state, the scattering angles of the top quark and top antiquark with respect to the jet direction are connected to their energies. Therefore, the effect of the charge asymmetry can be studied in terms of the energy asymmetry [6, 7] using the energy difference between the top quark and the top antiquark,  $\Delta E = E_t - E_{\bar{t}}$  and the production angle ( $\theta_j$ ) of the jet with the highest transverse momenta defined in the  $t\bar{t}j$  rest frame.

The main contribution to the energy asymmetry comes from  $gq \rightarrow t\bar{t}q$ . Here, the final-state-quark jet is boosted in the direction of the initial quark, which affects the rapidity of the  $t\bar{t}j$  system in the laboratory frame. Therefore, the optimised cross section,  $\sigma^{\text{opt}}(\theta_j)$ , is defined to optimise statistical sensitivity, combining forward events with positive rapidity of the  $t\bar{t}j$  system and backward events with negative rapidity of the  $t\bar{t}j$  system:

$$\sigma^{\text{opt}}(\theta_j) = \sigma(\theta_j | y_{t\bar{t}j} > 0) + \sigma(\pi - \theta_j | y_{t\bar{t}j} < 0), \quad \theta_j \in [0, \pi]. \quad (2)$$

Using the optimised cross section, the energy asymmetry ( $A_E$ ) can be defined as:

$$A_E(\theta_j) = \frac{\sigma_{E,A}}{\sigma_{E,S}} = \frac{\sigma^{\text{opt}}(\theta_j | \Delta E > 0) - \sigma^{\text{opt}}(\theta_j | \Delta E < 0)}{\sigma^{\text{opt}}(\theta_j | \Delta E > 0) + \sigma^{\text{opt}}(\theta_j | \Delta E < 0)}, \quad (3)$$

where  $\sigma_{E,S}$  and  $\sigma_{E,A}$  denote the charge-symmetric and charge-asymmetric cross-sections. The energy asymmetry increases with transverse momentum of the additional jet [7].